IOSR Journal Of Applied Physics (IOSR-JAP)
e-ISSN: 2278-4861.Volume 15, Issue 3 Ser. I (May. – June. 2023), PP 34-42
www.Iosrjournals.Org

Optimization Of A Solar Dryer: Study Of The Parameters Of The Solar Collector

MAMADOU SECK GUEYE [2], WALY FAYE [1, 2], OMAR NGOR THIAM [1], MAMADOU LAMINE SOW [1, 2]

1 Fluid Mechanics and Transfer Laboratory (MFT), Department of Physics, Faculty of Science and Technology, Cheikh ANTA DIOP University, Dakar-FANN, Senegal.
2 Research Group on Solar Energy and Transfers (GREST), Faculty of Science and Technology, Cheikh ANTA DIOP University (UCAD), Dakar, Senegal.

Abstract: *In this paper, a solar collector design model is developed based on some previous works published in the literature. Simplifying assumptions are made to simulate the behavior of the air flow at the inlet on the outlet temperature of the heat transfer fluid as a function of the glass-absorber gap and to choose the best gap for our sensor model. The thermo-physical coefficients of the sensor elements are taken from the literature. The numerical simulation results show that the model can be used to improve the operation of convective solar dryers. For this, the choice of the gap which gives the best performance is D=0.01m on a surface of 6m2 whose width is l=1.1m and length L=5.44m. We noted that the variations of the different temperatures become more and more very important, if the difference is smaller. For the proposed model with solar irradiation of less than 580W.m -2 , the solar drying of our reference product is possible with a reduced flow rate of 200m3 /h instead of 400m3 /h, obtained during dimensioning. We had as output temperature of the heat transfer fluid 343K or 70°C.*

Key Words: *Solar collector; Air flow; heat transfer fluid; convective solar dryers; solar irradiation*

Date of Submission: 04-05-2023 Date of Acceptance: 14-05-2023

I. INTRODUCTION

The applications based on the low temperature conversion of solar energy into thermal energy are numerous and diverse. These include solar heating of sanitary water, space heating and cooling, and solar drying of agricultural products [1].

Drying, an important operation in any processing of products from the food industry, is a very energy-intensive process. This explains the increasingly frequent use of renewable energies and mainly solar energy through the use of solar dryers [1].

Solar collectors are special cases of heat exchangers that convert solar energy into heat for low temperature applications. In solar dryers, the solar collector is useful to obtain high temperature values with controlled airflows. To have a better drying of the products with optimal conditions of temperature and air mass flow, it is necessary to ensure an optimal design of the solar collector [2].

Several parameters influence the thermal behavior of drying systems and therefore the efficiency and homogeneity of the products being dried. The experimental control of all these parameters is a very difficult and expensive task. To avoid the cost of experimental installations, many authors have proposed numerical models for solar dryers. These models have greatly contributed to the development of dryers, and to the prediction of their performance by increasing drying efficiency. Modeling techniques predict temperature, crop water content, drying rate and crop quality. Various modeling techniques have been used to analyze solar drying systems according to their global (thermodynamic modeling) or local (CFD calculation) nature [2].

Improving the thermal performance of solar collectors is based on several techniques which consist of:

Improve the absorber with new shapes of exchange surface to increase the absorbed heat flux and the heat exchange coefficient with the air.

Extend the travel time of the heat transfer fluid (air) by using multi-pass sensors.

This is why in this work we study the effect of the distance between glass and absorber to find the optimal opening for the passage of the heat transfer fluid; and the influence of the air flow at the inlet with the best distance (glass-absorber) to find the temperature admissible by the reference product at the outlet of the sensor.

II. MATHEMATICAL MODELING

To better understand the problem, some models have been studied:

- **Fluid outlet temperature model**

We can express, in general, the heat balance of a flat collector by equation (1). To simplify the study of heat transfers in the solar air collector, we use the method of analysis called nodal method i.e. cut the sensor into fictitious slices, from which we assume that:

- The air flow is unidirectional (along x),
- The thermal inertia of the heat transfer fluid is neglected,
- Lateral thermal losses of the collector are neglected,
- Temperatures of absorber, glass and insulator are uniform in a slice,
- Heat transfers between insulation and the outside air are neglected.

The heat equation in the heat transfer fluid is written: [3], [4], [5]

$$\mathbf{m_i Cp_i \frac{\partial T_i}{\partial t} + \overrightarrow{V_i} \overrightarrow{grad} \overrightarrow{Ti} = \sum h_{ij}\ S_{ij}(T_j - T_i) + \sigma_i} \qquad \mathbf{(1)}$$

In permanent mode, by neglecting the conduction in the fluid and by considering the flow which is carried out according to the coordinate (x), this equation (1) is written:

- **At glass level**

$$\rho_V\, v_v c_{p_v} \frac{dT_v}{dt} = S_c \alpha_v I_g + h_{rvam} S_c (T_{am} - T_v) + h_{VV} S_c (T_{am} - T_v) + h_{Cva} S_c (T_a - T_V) + h_{rabv} S_c (T_{ab} - T_v) \quad (2)$$

- **At the absorber**

$$\rho_{ab} v_{ab} c_{p_{ab}} \frac{dT_{ab}}{dt} = S_c \alpha_{ab} \tau_v I_g + S_c h_{rabv} (T_v - T_{ab}) + S_c h_{Caba} (T_a - T_{ab}) + S_c h_{Cdai} (T_{am} - T_{ab}) \quad (3)$$

at the level of the heat transfer fluid

$$Q_a\, c_{p_a} \Delta x \frac{dT_a}{dx} = h_{cva} S_c (T_v - T_a) + h_{Caba} S_c (T_{ab} - T_a) \quad (4)$$

III. CHARACTERISTIC PARAMETERS OF THE MODEL

Characteristic quantities and dimensionless quantities

To obtain dimensionless equations allowing a generalization of the study of the model, we used the following quantities:

L_C is the characteristic length of the sensor, $t_{se} = \frac{Q_{se}}{s_c L}$ is the reference time of the sensor and T_{sc}: is the characteristic temperature of the air at the outlet of the sensor.

$$\widetilde{T_a} = \frac{T_a}{T_{sc}} ; \widetilde{T_{ab}} = \frac{T_{ab}}{T_{sc}} ; \widetilde{T_v} = \frac{T_v}{T_{sc}} ; \qquad \tilde{t} = \frac{t}{t_{sc}} ; \tilde{x} = \frac{x}{L_c}$$

T_{se}: is again the characteristic temperature of the drying air, which indicates the end of drying. The drying time is the total duration of sunshine $t_{se} = 16 heuresis$ obtained in 2 days per 8 hours.

Dimensionless equations

From these reference quantities, we obtain the following dimensionless equations

- Energy balance at the glass (v)

$$\frac{d\widetilde{T_v}}{d\tilde{t}} = C_4 + C_1(\widetilde{T_{am}} - \widetilde{T_v}) + C_2 (T_a - \widetilde{T_v}) + C_3(T_{ab} - \widetilde{T_v}) \qquad (5)$$

$$C_1 = \frac{(h_{rvam} + h_{VV}) S_c t_{sc}}{\rho_v v_v c_{p_v}},\ \widetilde{T_{am}} = \frac{T_a}{T_{sc}} \qquad C_2 = \frac{h_{Cva} S_c t_{sc}}{\rho_v v_v c_{p_v}},\ C_3 = \frac{h_{rabv} S_c t_{sc}}{\rho_v v_v c_{p_v}},\ C_4 = \frac{S_c \alpha_v I_g t_{sc}}{T_{sc} \rho_v v_v c_{p_v}}$$

- Energy balance at the level of the absorber (ab)

$$\frac{d\widetilde{T_{ab}}}{d\tilde{t}} = C_8 + C_5(\widetilde{T_v} - \widetilde{T_{ab}}) + C_6(\widetilde{T_a} - \widetilde{T_{ab}}) + C_7(\widetilde{T_{am}} - \widetilde{T_{ab}}) \quad (6)$$

$$C_5 = \frac{h_{rabv} S_c t_{sc}}{\rho_{ab} v_{ab} c_{p_{ab}}},\ C_6 = \frac{h_{caba} S_c t_{sc}}{\rho_{ab} v_{ab} c_{p_{ab}}},\ C_7 = \frac{h_{cdai} S_c t_{sc}}{\rho_{ab} v_{ab} c_{p_{ab}}},\ C_8 = \frac{S_c \alpha_{ab} \tau_v I_g t_{sc}}{T_{sc} \rho_{ab} v_{ab} c_{p_{ab}}}$$

- Energy balance at the level of the heat transfer fluid (a)

$$\frac{d\widetilde{T_a}}{d\tilde{x}} = C_9(\widetilde{T_v} - \widetilde{T_a}) + C_{10}(\widetilde{T_{ab}} - \widetilde{T_a}) \qquad (7)$$

$$C_9 = \frac{h_{cva} S_c}{\Delta\tilde{x}\, Q_a\, c_{p_a}},\ C_{10} = \frac{h_{caba} S_c}{\Delta\tilde{x}\, Q_a\, c_{p_a}},$$

IV. CALCULATION OF SENSOR TRANSFER COEFFICIENTS

To determine the various heat exchange coefficients "h", the following relationships will be used, depending on whether it is a transfer by conduction, by convection or by radiation.

Assessment of h_{Cva} [6]

The determination of the coefficients h of heat exchange by convection is one of the areas which still pose problems in terms of heat transmission. Indeed, h is a coefficient which varies all along the surface in question. It is only possible to use an average coefficient. On the other hand, h depends on:

- geometric characteristics of the surface
- fluid characteristics
- the fluid flow regime (laminar/turbulent)
- from the definition of the temperature of the surface contact layer

If the flow of the fluid is due solely to the action of gravity, the convection is said to be natural or free. If this flow is imposed (pump, fan, etc.) convection is then said to be forced.

We are in this case. Let us agree to denote by v, the average wind speed and by Ta, the ambient temperature, then given that we are dealing with an external flow and seen elsewhere, the relative importance of the air exchange rate, we can evaluate the physical properties of the contact layer at Ta. Knowing the density, the dynamic viscosity coefficient and the thermal conductivity of the air evaluated at the reference temperature, we can calculate the Reynolds number, related to the length of the sensor and the prandtl number:

$$\mathbf{R_e = v.\frac{D_h}{\nu} = v.\rho\frac{D_h}{\mu}} \quad (8)$$

$$\mathbf{P_r = \mu\frac{c_p}{\lambda}} (9)$$

And hence $N_u = f(R_e, P_r)$ and finally:

$$\mathbf{h_{Cva} = h_{Caba} = N_u\frac{\lambda_a}{D_h}} (9)$$

The NUSSELT number is:

$$\mathbf{N_u = o,o196R_e^{o,8}.P_r^{1/3}} (10)$$

Convective exchanges due to the wind: these are the front losses due to the wind noted h_{VV}. According to the Hottel and Woertz correlation [7], the coefficient is described according to the following relationship:

$$\mathbf{h_{VV} = 5,67 + 3,86\ u_a} \quad (11)$$

Radiation exchange coefficients [8]

The elements that make up the flat air collectors (glazing, absorber and insulation) most often have a rectangular shape. All these surfaces are parallel and the distances which separate them are small. This allows us to simplify the form factors and take the average temperatures of the elements in order to express the radiative coefficients. For this we often use the following classic formulation:

$$\mathbf{h_r = \frac{\sigma(T_1 + T_2)(T^2{}_1 + T^2{}_2)}{\frac{1-\varepsilon_1}{\varepsilon_1} + \frac{1}{F_{12}} + \frac{1-\varepsilon_2}{\varepsilon_2}(\frac{S_1}{S_2})}} \quad (12)$$

a) Radiative exchange between the glass and the ambient environment

This exchange coefficient is given by the relation

$$\mathbf{h_{rvam} = \sigma\,\varepsilon_V\frac{(1-\cos\alpha)}{2}(T_V + T_{am})(T^2{}_V + T^2{}_{am})} \quad (13)$$

b) Radiative exchange between the glass and the absorber

$$\mathbf{h_{rabv} = \frac{\sigma(T_V + T_{ab})(T^2{}_V + T^2{}_{ab})}{\frac{1}{\varepsilon_V} + \frac{1}{\varepsilon_{ab}} - 1}} \quad (14)$$

Exchanges by conduction

For our case we will take into account the losses by conduction between the absorber and the insulator

$$\mathbf{h_{cdabi} = \frac{e_{ab}}{\lambda_{ab}} + \frac{e_{air}}{\lambda_{air}} + \frac{e_{is}}{\lambda_{is}}} \quad (15)$$

V. DISCRETIZED EQUATIONS [9], [10], [11]

The heat transfer equations (5) (6) and (7) described are nonlinear and coupled partial differential equations. Due to their complexity, these equations are solved by numerical techniques. The spatial discretization is done by a finite difference method while a purely implicit scheme is adopted for the temporal discretization [9]. The equations discretized according to their level are:

- Energy balance at the glass (v)

$$\frac{\tilde{\mathbf{T}}^{\mathbf{t}}_{\mathbf{v(i)}} - \tilde{\mathbf{T}}^{\mathbf{t-\Delta t}}_{\mathbf{v(i)}}}{\mathbf{\Delta \tilde{t}}} = \mathbf{C_4} + \mathbf{C_1}(\tilde{\mathbf{T}}_{\mathbf{am}} - \tilde{\mathbf{T}}^{\mathbf{t}}_{\mathbf{v(i)}}) + \mathbf{C_2}(\tilde{\mathbf{T}}^{\mathbf{t}}_{\mathbf{a(i)}} - \tilde{\mathbf{T}}^{\mathbf{t}}_{\mathbf{v(i)}}) + \mathbf{C_3}(\tilde{\mathbf{T}}^{\mathbf{t}}_{\mathbf{ab(i)}} - \tilde{\mathbf{T}}^{\mathbf{t}}_{\mathbf{v(i)}}) \qquad (\mathbf{16})$$

- Energy balance at the level of the absorber (ab)

$$\frac{\tilde{\mathbf{T}}^{\mathbf{t}}_{\mathbf{ab(i)}} - \tilde{\mathbf{T}}^{\mathbf{t-\Delta t}}_{\mathbf{ab(i)}}}{\mathbf{\Delta \tilde{t}}} = \mathbf{C_8} + \mathbf{C_5}(\tilde{\mathbf{T}}^{\mathbf{t}}_{\mathbf{v(i)}} - \tilde{\mathbf{T}}^{\mathbf{t}}_{\mathbf{ab(i)}}) + \mathbf{C_6}(\tilde{\mathbf{T}}^{\mathbf{t}}_{\mathbf{a(i)}} - \tilde{\mathbf{T}}^{\mathbf{t}}_{\mathbf{ab(i)}}) + \mathbf{C_7}(\tilde{\mathbf{T}}_{\mathbf{am}} - \tilde{\mathbf{T}}^{\mathbf{t}}_{\mathbf{ab(i)}}) \qquad (\mathbf{17})$$

- Energy balance at the level of the heat transfer fluid (a)

$$\frac{\tilde{\mathbf{T}}^{\mathbf{t}}_{\mathbf{a(i)}} - \tilde{\mathbf{T}}^{\mathbf{t}}_{\mathbf{a(i-1)}}}{\mathbf{\Delta \tilde{X}}} = \mathbf{C_9}(\tilde{\mathbf{T}}^{\mathbf{t}}_{\mathbf{v(i)}} - \tilde{\mathbf{T}}^{\mathbf{t}}_{\mathbf{a(i)}}) + \mathbf{C_{10}}(\tilde{\mathbf{T}}^{\mathbf{t}}_{\mathbf{ab(i)}} - \tilde{\mathbf{T}}^{\mathbf{t}}_{\mathbf{a(i)}}) \qquad (18)$$

The iterative process is repeated until there is no longer any significant change in the value of F with respect to the following convergence criterion:

$$\frac{\sum \left| F^{n+1} - F^{n} \right|}{\sum \left| F^{n+1} \right|} \leq \varepsilon_r \qquad (19)$$

With ε_r is the calculation precision.

VI. INPUT DATA FOR COMPUTER CODE

Table no 1: Effect of the Variation in the Glass-Absorber Distance

Distance Glass opening – absorber(m)	0.01	0.02	0.03	0.04	0.05	0.06	0.07	0.08	0.09	0.1
Reynolds number	**3.5310 6**	**1.7610 6**	**1.1710 6**	**8.7410 5**	**6.991 0 5**	**5.9410 5**	**5.0410 5**	**4 .5410 5**	**3 .9210 5**	**3.5310 5**
Number of NUSSELS	**3058.7**	**1756.7**	**1270.1**	**1000.9**	**837.3**	**735.2**	**644.8**	**593.2**	**527.4**	**484.8**
Convection coefficient (Wm -1 .k -1)	**14.6**	**8.4**	**6.1**	**4.8**	**4.0**	**3.5**	**3.1**	**2.8**	**2.5**	**2.3**
Air speed (m/s)	**10.1**	**5.1**	**3.4**	**2.5**	**2.0**	**1.7**	**1.4**	**1.3**	**1.1**	**1.0**

Table **no** 1 was obtained by choosing the absorber glass gap to calculate parameters such as: the convection coefficient, the Reynolds and NUSSELT number and the air sweep speed.

For this Table, the inlet flow rate has been set at 400m ^{3} /h for the model of collector dimensioned.

So what will allow us to obtain the results on the Effect of the Variation of the Glass-absorber gap. In order to choose the best difference which gives the outlet temperature admissible by the product to be dried.

- Turbulent flow

$\mathbf{N_u = o,o196 R_e^{o,8}.P_r^{1/3}}$; We have $\mathbf{P_r = 0.73}$ $\mathbf{R_e}$ >510 5 **et** $\mathbf{P_r \geq 0.5}$ **(20)**

- Laminar flow

$\mathbf{N_u = o,o196 R_e^{o,8}.P_r^{1/3}}$ $\mathbf{R_e}$ <510 5 **et** $\mathbf{10 \geq P_r \geq 0.5}$ **(21)**

Table no 2: the effect of the variation in the air flow on the temperature of the heat transfer fluid at the outlet of the sensor

Air flow (m ^{3} /h)	200	400	800	1000
Reynolds number	**1.7610 6**	**3.5310 6**	**7.0610 6**	**8.8210 6**
Number of NUSSELS	**1756.7**	**3058.7**	**5325.0**	**6365 .7**
Convection coefficient (W .m $^{-1}$ .k $^{-1}$)	**8.4**	**14.6**	**25.5**	**30.4**
Airspeed (m/s)	**5.05**	**10.10**	**20.20**	**25 .25**

This second table repeats the same calculations of the coefficients as table 1 while varying the air flow at the entrance. The results obtained make it possible to know the effect of the variation of the air flow on the temperature of the heat transfer fluid at the outlet of the sensor.

The objective is to be able to size a model of solar dryer capable of operating under unfavorable conditions. That is, being able to come up with a model that could work in low sunlight conditions.

VII. RESULTS AND DISCUSSION

Effect of the variation of the glass-absorber gap on the temperature of the heat transfer fluid

We have varied the distance between glass and absorber:

- $D_1 = 0.01$ ($T_{absorber1}$ _____ T_{air1} _____ T_{glass1})
- $D_2 = 0.02$ ($T_{absorber2}$ _____ T_{air2} _____ $T_{glass\ 2}$)
- $D_3 = 0.03$ ($T_{absorber3}$ _____ T_{air3} _____ $T_{glass\ 3}$)
- $D_4 = 0.04$ ($T_{absorber4}$ _____ T_{air4} _____ $T_{glass\ 4}$)
- $D_5 = 0.05$ ($T_{absorber5}$ _____ T_{air5} _____ T_{glass5})
- $D_6 = 0.06$ ($T_{absorber6}$ _____ T_{air6} _____ $T_{glass\ 6}$)
- $D_7 = 0.07$ ($T_{absorber7}$ _____ T_{air7} _____ $T_{glass\ 7}$)
- $D_8 = 0.08$ ($T_{absorber8}$ _____ T_{air8} _____ $T_{glass\ 8}$)
- $D_9 = 0.09$ ($T_{absorber9}$ _____ T_{air9} _____ T_{glass9})
- $D_{10} = 0.1$ ($T_{absorber10}$ _____ T_{air10} _____ $T_{glass10}$)

It is observed at the first instants that the variations of the different temperatures (absorbers-heat transfer fluids-glass) decrease according to the progression at the first positions in the sensor for any difference between glass and absorber.

At the last positions, these variations are different depending on the glass-absorber distance considered for the glass and heat transfer fluid temperatures (figures 1b and 1c) and a little confused for the absorber temperatures (figure 1a).

It is concluded that the fact of varying the gap (glass-absorber) of passage of the air has no remarkable effect on the variations of the temperature of the absorber at the first instants. But also, does not allow to also have the outlet temperature of the desired heat transfer fluid depending on the position. It can be seen that from the first passages of the air, for any difference considered, the glass and fluid temperatures decrease according to the position. Because as the air progresses, the exchange of matter between air and glass or absorber (convection) increases, hence the temperatures decrease.

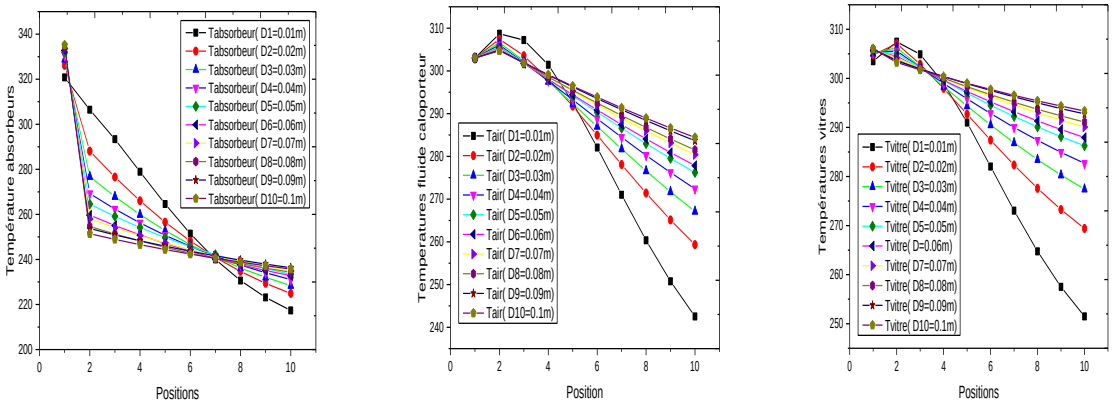

(1a) (1b) (1c)

Fig1: Variation of the Temperatures of the different Elements at the first moments of passage of the air according to the displacement

At several passages of the air, it is noted that the variations in the temperatures of the glass and air evolve according to the positions in greater ways than those of the absorbers.

By comparing these evolutions according to the passage distance, we notice from the third position the variations of the glass and fluid temperatures (figures 2b and 2c) are greater for a distance D_1=0.01m compared to the other D_2= 0.02, D_3=0.03, D_4=0.04, D_5=0.05, D_6=0.06, D_7=0.07, D_8=0.08, D_9=0.09, D_{10}=0.1. Whose temperature order is at T_{air}=321K and T_{glass}=315K.

At the first position, the temperature of the absorber is greater if the gap is 0.1. At positions 2 and 3 for the differences D2….D10 the different temperatures increase then decrease from the 4th position progressively according to the displacement. Contrary to D1, there is a more significant evolution up to the 4th position then gradually decreases like the differences considered (figure 2a).

It is interpreted that the glass-absorber gap, the smallest, gives the best variations in the glass and fluid temperatures. This is due to the fact that the losses by conduction are less important compared to the effects by convection. Hence the Reynolds number relative to the length of the sensor increases if the glass-absorber gap decreases.

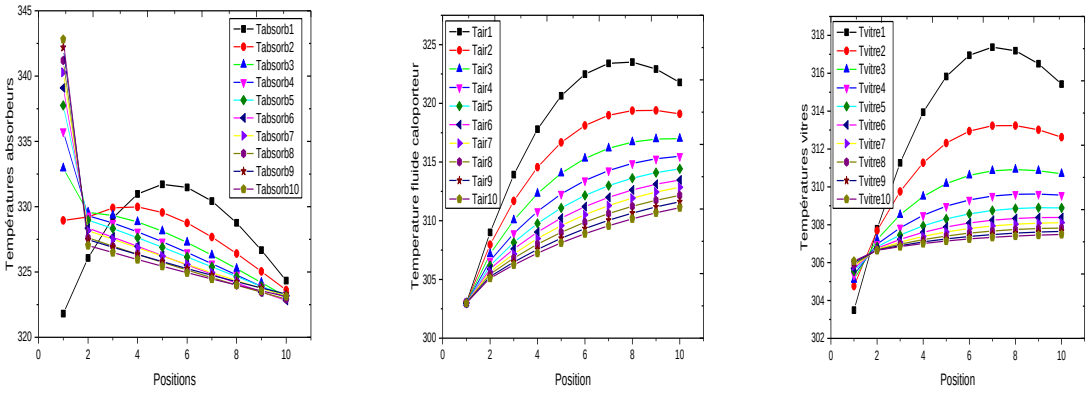

(2a) (2b) (2c)

Fig2: Variation of the Temperatures of the different Elements with several passages of the air according to the Positions

Figures 3a, 3b, 3c, 3d, 3e…3j show the variations of the different temperatures at the outlet of the sensor taken at the last moments of passage of the heat transfer fluid.

These different figures have just confirmed the results of figures 2a, 2b and 2c. For each case of difference considered, the temperature of the absorber is much higher than that of the other two.

So we confirm the following phenomenon: the smaller the glass-absorber gap, the greater the temperature variations become. This is what we observe in figure 3a, which corresponds to D=0.01m. With this distance, the air temperature reaches 333K at the last position, i.e. 60°C for an irradiation considered at 500 W.m $^{-2}$ with an input flow rate of 400 m ^{3} /h.

For the window and absorber temperatures, we have 325K and 346K respectively.

Conclusion: The best difference that gives the outlet temperature closest to that of the product to be dried is D1. According to our model, it is the drying temperature that corresponds to the heating time or first phase of drying.

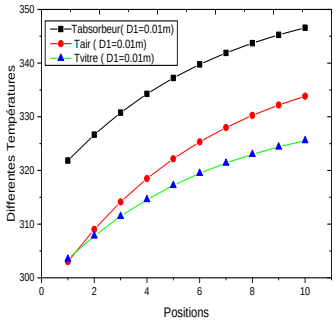

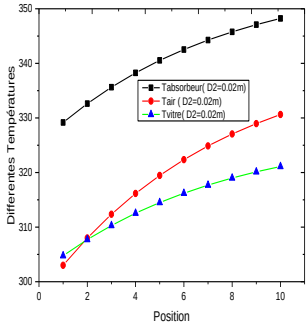

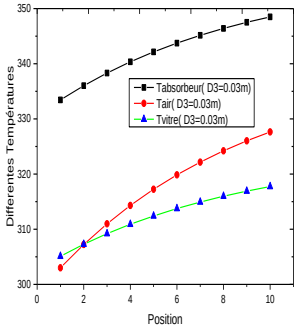

(3a) (3b) (3c)

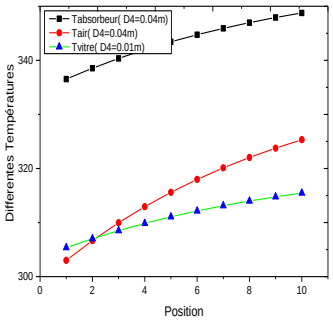

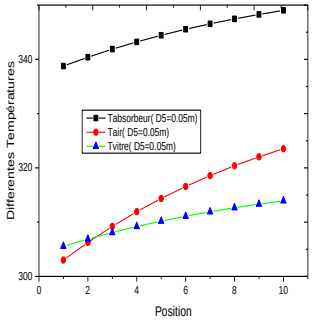

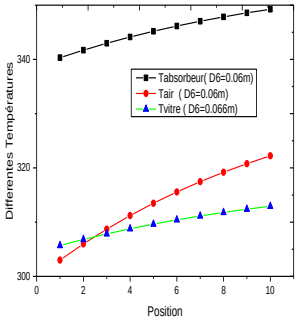

(3d) 3(e) (3f)

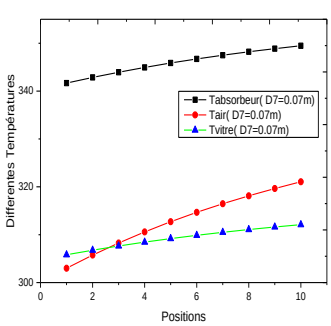

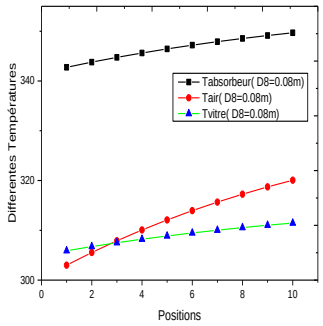

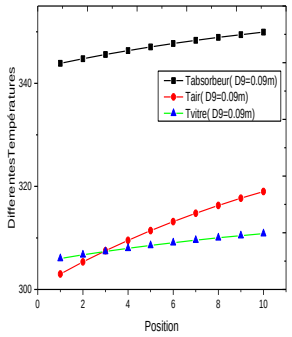

(3g) 3(h) (3i)

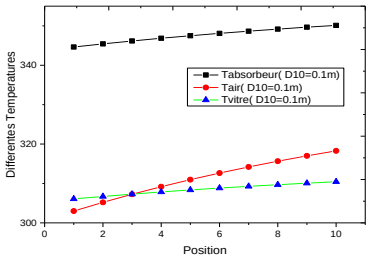

(3d)

Fig3: Variation of the Temperatures of the different Elements at the last moments of the passage of the air according to the Positions

Effect of the variation of the air flow on the temperature of the heat transfer fluid at the outlet of the sensor

For these results, we try to see the influence of the variation of the air flow on the best gap chosen.

Figures 4a, 4b, 4c successively show us the variations of the temperature of the fluid at the beginning, in the middle and at the end.

At the beginning, we observe from the 4th position the variations of the temperatures of the fluid decrease gradually between 300K and 250K.

In the long time, the air temperatures increase according to the position for the cases of flow considered. Except for the difference D_1 where we observe from the sixth position the variations of the air temperature decreases.

At the exit, these variations become more significant and increase as a function of the position for the flow cases considered. As these variations are greater when the flow rate is low at 200m ^{3} /h.

We note at 200m ^{3} /h, we reach the outlet fluid temperature is 337K or 64°C.

For 400 m ^{3} /h, 800 m ^{3} /h and 1000 m ^{3} /h, we obtain as heat transfer temperature respectively 333K, 326K finally 323K. Or again respectively 60°C, 53°C and 50°C for a radiation of 500W.m -2 .

These results allow us to see with the chosen glass-absorber gap, the smaller the considered inlet flow rate, the more the temperature variations increase.

When the inlet flow is high the outlet temperature decreases depending on the position. This will allow us to properly control the last drying phase called the bound water extraction phase. So increasing the flow means decreasing the air temperature.

Conclusion: With an input flow of 200m^3/h and radiation of 580W.m^{-2}, we reached an output temperature of 70°C. While the objective was to reach a temperature of 70°C to assume that the product is well dried.
So with our proposed model at 580W.m^{-2} of radiation, solar drying of our product is feasible.

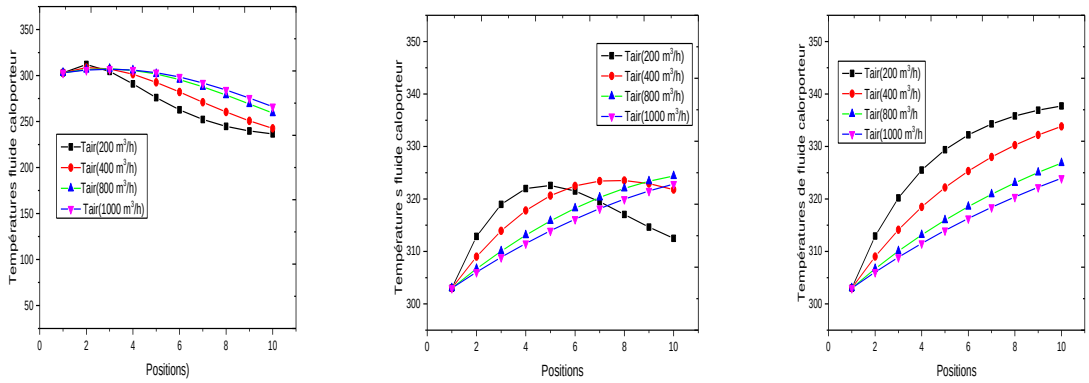

4(a) **4(b)** **4(c)**

Fig4: Effect of flow on the temperature of the heat transfer fluid along the sensor

VIII. CONCUSION

In sum, this study focused on the proposal of a mathematical model that highlights the parameters of the solar collector. This model, based on the Navier Stokes equations, allowed us to study the phenomena of convection, conduction and radiation which govern the heat transfer equations of the sensor elements.

By taking into account the geometry model, we were able to establish the equations and perform the calculation of the parameters of the various coefficients. To validate the method used, the objective was to study the effect of the variation of the glass-absorber gap and the variation of the air flow on the temperature of the heat transfer fluid at the outlet of the sensor as a function of the displacement.

The results obtained allowed us to confirm that the best difference for the performance of our sensor is as small as possible. It turned out that the glass-absorber distance 0.01m gives the greatest outlet temperature of the heat transfer. For an air flow of 200m 3 /h, this temperature is around 343K, i.e. 70°C.

References

[1]. Said, Tebbane Ahmed Laraba, Design and construction of a solar dryer using an aerovoltaic system for drying food products, MOHAMEDBOUDIAF-M'SILA UNIVERSITY, 2022
[2]. https://www.rapport-gratuit.com/modelisation-mathematique-des-sechoirs-solaires/ ; visited on 01/11/2023
[3]. Benlahmidi Said, Study of convective drying by solar energy products red, PhD Thesis, University Mohamed Khider-Biskra, 2013.
[4]. S.El Mokretar , R.Miri , and M.Belhamel , Energy balance and mass Study of a greenhouse type of dryer for drying applications Food products, Development Center Of Review Of Renewable Energy.Vol.7 (2004) pp. 41-48.
[5]. Boubeghal , M. Benhammou , B. Omari S. Amara L. Amer , H. Moungar and S. Ouejdi , Numerical study of a solar dryer running in natural convection Journal of Renewable Energies ICRESD-07 Tlemcen (2007) 315 - 320.
[6]. Ndiaye, Aly Ngduille, Modeling of a Solar System with an Empty Tube Collector, Ecole Polytechnique de THIES, 1996
[7]. Daguenet, M. (1985). Solar dryers: theory and practice. UNESCO Publication, Paris, France, 320-325
[8]. M.Kouhila, and Kane, CSE. (2006). Experimental study of the convective drying of sage in a solar dryer equipped with an electric back-up, Proceedings 1st Magrébin seminar on the Sciences and Technologies of Drying, 301-306.
[9]. Mamadou Seck Gueye, Omar Ngor Thiam , Samba Dia , Joseph Sarr . (2014). Description of the Temperature in an Indirect Solar Dryer: Application in the Drying of the ' Niebe ' International Journal of Engineering Application (IREA), vol (2): 123-128
[10]. Goncalvès, E. (2005), Numerical Resolution Discretization of PDEs and ODEs, Institut National Polytechnique De Grenoble.
[11]. Euvrard, D. (1990). Numerical resolution of partial differential equations, physics, mechanics and engineering sciences , finite differences, finite element, singularity method. Masson Paris pub, 2nd Ed.